Tian et al. *Zool. Res.* 2025, 46(2): 370−378
https://doi.org/10.24272/j.issn.2095-8137.2024.314
https://cstr.cn/32248.14.zr.2024.314

ZR Zoological Research

Article Open Access

Bilateral asymmetry in craniofacial structures and kinematics of feeding attacks in the scale-eating cichlid fish, *Perissodus microlepis*

Xiaomeng Tian[1], Sooyeon Lee[2], Jan Tuckermann[2], Axel Meyer[1,3,4,*]

[1] *Department of Biology*, *University of Konstanz*, *Konstanz* 78464, *Germany*
[2] *Institute of Comparative Molecular Endocrinology*, *Ulm University*, *Ulm* 89081, *Germany*
[3] *Museum of Comparative Zoology*, *Harvard University*, *Cambridge*, *MA* 02138, *USA*
[4] *CAS Key Laboratory of Tropical Marine Bio-Resources and Ecology*, *South China Sea Institute of Oceanology*, *Chinese Academy of Sciences*, *Guangzhou*, *Guangdong* 510301, *China*

ABSTRACT

Cichlid fishes are a textbook example for adaptive radiations, since they diversified into several hundred highly specialized species in each of three great East African lakes. Even scale-eating, an extremely specialized feeding mode, evolved independently multiple times in these radiations and in Lake Tanganyika alone, six endemic scale-eating species occupy this extremely specialized ecological niche. *Perissodus microlepis* went a step further, by evolving bilaterally asymmetrical heads with an intra-specific polymorphism where left- and right-headed morphs predominantly scrape scales from the opposite sides of their prey. While the bilateral asymmetry of scale-eating cichlids has been known, exactly which craniofacial features explain the laterality of the heads remained unclear. Here we aimed, by utilizing micro-computed tomography (µCT), to resolve this issue of how bilateral symmetry in the skeletal structure is broken in scale-eating *Perissodus*. Our 3D geometric morphometrics analysis clearly separated and identified the two groups of either left- or right-headed fish. In addition, we observed consistent asymmetric volume changes in the premaxilla, maxilla, and mandible of the craniofacial structures, where left-headed fish have larger jaw elements on the right side, and vice versa. The bimodality implies that the effect sizes of environmental factors might be minor while genetics might be responsible to a larger extent for the asymmetry observed in their head morphology. High-speed video analyses of attacks by asymmetrical morphotypes revealed that they utilize their asymmetrical mouth protrusion, as well as lateralized behavior, to re-orientate the gape towards the preferred side of their prey fish to more efficiently scrape scales.

Keywords: Cichlids; Geometricmorphology; Asymmetry; Micro-computed tomography

INTRODUCTION

Cichlid fishes are a prime example for rapid adaptive morphological diversification and the Cichlidae is one of the most species-rich families of vertebrates. The evolutionary success of cichlids has been attributed, at least in part, to their innovative cranial system and the de-coupling of their oral and pharyngeal jaws (Liem, 1973), as well as their variability in foraging and complex social behaviors (Keenleyside, 1991). Recently, it was proposed that their curiosity might have allowed them, more than other fish, to explore ecological opportunities seeking novel habitats and exploit new ecological niches (Sommer-Trembo et al., 2024). *Perissodus microlepis*, in particular, a scale-eating cichlid species endemic to Lake Tanganyika, has been cited as a textbook example for these evolutionary processes (Futuyma, 2009). Its asymmetric head, associated with lateralized foraging behavior equips it to exploit a particularly narrow ecological niche especially efficiently —in this case, foraging on the scales of other (cichlid) fish species, since they are specialized to feed predominantly from either the right or the left sides of their preys based on the asymmetric head morph (Hori, 1993; Lee et al., 2017). In this species, two morphotypes can be recognized: The left-headed (L) and the right-headed (R) (Hori, 1993). The first morph predominantly feeds on the right side of their prey, while the latter morph exhibits the opposite preference. When populations are surveyed for several years a long-term ratio of nearly 50:50

Received: 20 September 2024; Accepted: 03 December 2024; Online: 04 December 2024

Foundation items: This work was principally supported by Deutsche Forschungsgemeinschaft grant to A.M., a Hector Fellow Academy Ph.D. fellowship and Jim Smith Endowment Fund Grant of the Ohio Cichlid Association to X.T., and Deutsche Forschungsgemeinschaft grant to J.T.

*Corresponding author, E-mail: axel.meyer@uni-konstanz.de

was observed (Hori, 1993; Kusche et al., 2012; Lee et al., 2010). Interestingly, that 50:50 ratio was not strictly adhered to every year, but rather fluctuated and cycled back within approximately four to five years (Hori, 1993). This cyclic frequency change of the abundance of the right- and left-morph has been interpreted as being caused by negative frequency-dependent selection (Hori, 1993; Kusche et al., 2012) as the more abundant morph would be selected against (due to being detected more readily by their prey fish, that survive and presumably remember these attacks that would be more frequent from one particular side) thereby favoring the predation success of the less common morph, leading to their higher fitness and resulting in a subsequent increase in relative abundance of the more rare morph (Berlinghieri et al., 2021; Lee et al., 2010). This negative frequency-dependent model requires that some portion of the left-right headedness of these fish must be heritable (Lee et al., 2010, 2015). Bilateral asymmetry, as a stable deviation from the widely prevalent symmetry patterns in evolutionary and developmental biology, holds profound and important significance different from other symmetry deviations (Levin, 2005), like fluctuating asymmetry (Nijhout & Davidowitz, 2003) and directional asymmetry (Pither & Taylor, 2000). As a result, considerable research has been devoted to investigating the genetic basis of its bilateral morphological asymmetry (Lee et al., 2017; Raffini et al., 2017, 2018; Stewart & Albertson, 2010; Takeuchi et al., 2018).

Many biological aspects of the head asymmetry in *P. microlepis* still remain poorly understood. For example, it is unclear exactly which osteological traits cause the lateral head asymmetry. Liem & Stewart (1976) were the first to attempt to understand which bones were bringing about the lateral asymmetry, but did not reach conclusive results. It had also been noted that different populations of this scale-eating cichlid in Lake Tanganyika exhibit distinct patterns of asymmetry: some populations display a bimodal bilateral asymmetry (Hori, 1993; Hori et al., 2007), while others exhibit a more continuous distribution (Kusche et al., 2012). The morphs are quite easily identified when freshly caught in the field by viewing the fish from above, as first described by Hori (Hori, 1993) and others (Kusche et al., 2012; Lee et al., 2010; Takeuchi et al., 2012). Based on this technique, *P. microlepis* R-morphs are characterized by the ascending process of their premaxillary bone being oriented towards the right, and to the opposite side for the L-morphs (Kusche et al., 2012). Later Kusche et al. (2012) using dorsal view *P. microlepis* photographs, digitally measured the bending angles of both morphs by connecting the eye sockets and the tip of the snout (hereafter referred to as “dorsal photograph” technique). In contrast to measurements on soft tissue, isolation of specific craniofacial bones such as the mandible (Hata et al., 2013), and the use of X-rays (hereafter referred to as “X-ray imaging”) (Indermaur et al., 2018) were also applied to these cichlids, to more objectively quantify internal skeletons, and to increase the accuracy for a more confidential determination of the L- or R- morphs in preserved specimens.

Different approaches did not always yield the same consistent distributions of L- and R-morphs, but reliable and repeatable phenotyping is necessary for accurate studies of this fish including heritability estimations. A discrete/bimodal distribution of head asymmetry may suggest a relatively simple Mendelian/oligogenic basis for the head asymmetry (Hata et al., 2013; Hori, 1993). Conversely, a continuous unimodal distribution would indicate a more complex (polygenic) genetic architecture and potentially suggest a stronger influence of non-genetic factors such as phenotypic plasticity (Lee et al., 2015; Van Dooren et al., 2010). Many of these crucial issues remain unanswered including a more accurate description of the asymmetric head morphology to begin with. Since this involves working with preserved specimens, it is important to account for the effects of fixation in formalin or ethanol on accurate morphotype quantification. Additionally, how this bilateral asymmetrical craniofacial morphology is involved in scale-eating behavior in live fish needs further investigation. The goal of this study is to address these morphological issues in *Perissodus* to enhance the understanding of this notable case of bilateral asymmetry and the maintenance of its trophic polymorphism.

The lateralized behavior, coupled with the asymmetric morphology, facilitates the exploration and specialization of fish scales as food source even from only one or the other side of their prey in this species (Raffini & Meyer, 2019; Takahashi et al., 2007; Takeuchi et al., 2016). While observations of lateralized feeding exist for these fish from both nature (Hori, 1993; Kawano et al., 1987) and laboratory settings (Lee et al., 2012; Takeuchi et al., 2019, 2022; Van Dooren et al., 2010), many gaps in knowledge remain. Takeuchi et al. (2022) documented the lateral-feeding behavior in the laboratory, by high-speed filming. The fish also consume other diets such as conventional fish food in laboratory although they seem to prefer to eat scales. Nonetheless, crucial information such as how the mouth protrusion might be adjusted by the fish when feeding on different diets has not been quantified due to limitations in resolution (e.g., the number of pixels) in high-speed filming (Takeuchi et al., 2022; Takeuchi & Oda, 2017). Lateralized predation and craniofacial asymmetry presumably arose due to intense competition (Hori, 1993).

We quantified the asymmetric craniofacial structure in *P. microlepis* in an effort to better understand which changes contribute to the asymmetry, thereby increasing the fishes’ ability to feed laterally on scales. First, we assessed existing methods for quantifying L- and R- morph. Moreover, we introduced high-resolution micro-computed tomography (μCT) to quantitatively measure asymmetry in 3D craniofacial skeletons (refer to “3D μCT”) and employed high-speed imaging to detail jaw kinematics during feeding on different types of food. Our study offers an unbiased way to measure head asymmetry, linking phenotype to behavior, and serves as a basis for further research on phenotype-genotype connections in the skeletal system.

MATERIALS AND METHODS

Field sampling of specimens

In April 2018, 102 wild-caught *P. microlepis* specimens were collected from five locations in Zambia (Supplementary Table S1), following local regulations and guidelines (Kusche et al., 2012; Permit G. R. no: 2077761). The specimens' standard lengths ranged from 3.8 to 9.4 cm, averaging 6.8 cm.

Field examination

The L- and R-morphs in 102 freshly caught *P. microlepis* were visually determined in the field based on Hori (1993) criteria. L-morph had a premaxilla ascending process oriented to the left, while R-morph had them pointing in the opposite direction.

After examination, all the specimens were preserved in 98% ethanol and stored at 4°C for further studies. A chi-square test (Pearson, 1900) was performed to evaluate the expected 50:50 ratio of L- and R- morphs.

Dorsal photograph

In the laboratory, all 102 ethanol-preserved *P. microlepis* were photographed from dorsal using a Panasonic Lumix DMC-FZ72 camera (Panasonic, Japan). The mouth asymmetry was measured by marking three landmarks on the eye sockets and the snout, following Raffini et al. (2017) and then quantified as the difference between left (αL) and right (βR) angles, with positive values indicating L-morph and negative for R-morph. Measurement repeatability was verified using a double-blind method on 20 individuals. The analysis was conducted using tpsDig (Rohlf, 2006a), tpsUtil (Rohlf , 2006b), and Python (Van Rossum & Drake, 2009).

X-ray image determination

Bilateral asymmetry of the internal skeleton in the same 102 specimens was quantified using the premaxilla-vertebrae angle derived from X-ray images. Specifically, dorsal-ventral X-ray images of each head were taken with a ZooMax Digital X-ray machine (Control-X Medical, USA) at 52 kVp peak and 4-7 mAs for optimal resolution. The degree was calculated as the angle θ between the line from the first two vertebrae and the line from the middle of otoliths to the premaxilla tip. Positive θ values indicated L-morph, while negative values indicated R-morph.

3D μCT

Based on the X-ray-derived bending angles, we selected 20 individuals with extreme asymmetry (*n*=10 L, *n*=10 R) and 20 with nearly symmetrical heads (*n*=20) for detailed 3D skeletal measurements. The μCT scans were conducted at the University of Ulm using a Skyscan 1176 (Bruker, Belgium). The scanner settings were: isotropic voxel resolution of 18 μm, X-ray voltage of 50 kV, current of 500 μA, a 0.05 mm aluminum filter, and a 1° rotation step. The resulting images were reconstructed using NRecon software (Bruker, Belgium) and processed with 3D Slicer (Fedorov et al., 2012).

Three craniofacial skeletal elements —the premaxilla, maxilla, mandible, which directly contact prey during scale-eating (see feeding videos below) and can be clearly separated were further examined. These elements were isolated to measure relative volume, density, and shape variation. Suspensorium, though potentially informative, was not included in the volume and density comparison due to insufficient ossification in some areas but were included in the subsequent geometric analysis. The relative volumetric asymmetries between left and right sides were calculated based on the following equation (Palmer & Strobeck, 1986).

$$\text{Degree of asymmetry} = (\text{Left} - \text{Right})/(\text{Left} + \text{Right}) \qquad (1)$$

Bone density was represented by the average Hounsfield Units (HU), calculated using the Segment Statistics module on the segmented bones. Density asymmetries were computed using the same equation as described above. Geometric morphometrics (GM) analysis involved placing 96 landmarks on homologous and anatomically recognizable features on both sides of the head (Supplementary Figure S1). Major 3D shape variations among the specimens were extracted using generalized Procrustes analysis (GPA) (Gower, 1975; Rohlf & Slice, 1990) and then summarized with principal component analysis (PCA) (Pearson, 1901). Asymmetric levels were calculated using the relative volume ratio between the left and right sides or the resulting PCs.

The impact of mouth posture during fish preservation was eliminated by removing the variation in PC1: First, we standardized the landmarks using GPA for scaling and rotation. We then performed PCA on the standardized landmarks to obtain the PCs and their load and score matrices. To eliminate the influence of PC1 on the dataset, we nullified its impact using a specific equation, thereby correcting PC1's effects in the initial PCA analysis (equation below).

$$X_{\mathrm{corr}} = X - s1 \times v1{}^{\wedge}\mathrm{T} \qquad (2)$$

where X_{corr} is the adjusted landmark matrix, X is the original landmark matrix, *s1* is the score vector of PC1, *v1* is the load vector of PC1, and ^T is transposition of the vector.

High-speed videography and digitizing

Wild-caught *P. microlepis* were used to study feeding kinematics on goldfish scales or non-scaly food. The experiments were conducted in a 50 cm long×25 cm wide×30 cm high tank filled with 25 liters of water. High-speed videos were recorded at 400 frames per second (fps) and 1920×1080 pixels using a Sony NEX-FS700R camera (Sony, Japan) positioned 20 cm above the tank. The tank background featured a 1 cm² grid for contrast and length estimation. The camera was remotely operated to minimize interference. Specimens were acclimated in the tank for one day before the experiments. During scale-eating trials, a goldfish was introduced into the tank corner without human presence while recording. For non-scaly food trials, mysis shrimp were gently dropped into the tank, allowing the fish to eat as they fell.

RESULTS

Inconsistencies in three conventional phenotypic measurements

Three conventional methods were used in this study to evaluate head asymmetry. We first visually inspected the 102 freshly caught *P. microlepis* in the wild, identifying 50 samples as L-morph, 48 samples as R-morph, and four as indeterminant due to their ambiguous morphology. The L- and R-morph ratios met the expected 50:50 distribution (χ^2 test, *P*-value>0.05). Using the "dorsal photograph" methodology based on mouth-bending angles, 60 samples were classified as L-morph and 42 samples as R-morph and met the 50:50 expectation (χ^2 test, *P*-value>0.05), with a continuous and unimodal distribution (Figure 1A). Moreover, the X-ray-derived skeleton asymmetry also yielded a unimodal distribution (Figure 1B). Among the 102 specimens, 43 were identified as L-morph and 59 as R-morph, with no significant deviation from a 50:50 ratio (χ^2 test, *P*-value>0.05). However, the morph classification was clearly inconsistent among "field examination", "dorsal photograph", and "X-ray imaging" methods ("field examination" vs. "dorsal photograph": T-test, *P*-value>0.05, Figure 1C; "field examination" vs. "X-ray imaging": T-test, *P*-value>0.05; Figure 1D; "dorsal photograph" vs. "X-ray imaging": Pearson correlation, r=0.07, *P*-value> 0.05; Figure 1E).

μCT adoption addressed inconsistencies

We next conducted μCT measurements to address potential inconsistencies among the three earlier methods. Our μCT

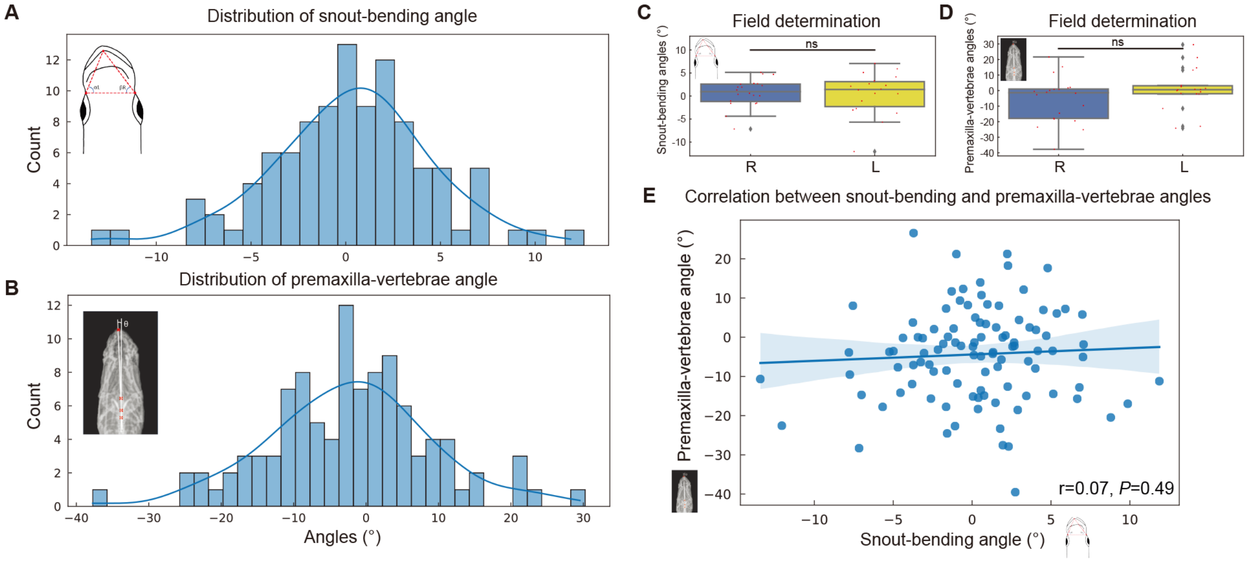

Figure 1 Frequency distribution of head asymmetry in *Perissodus microlepis*

A: Distribution of snout-bending angle of 102 fish (dorsal photograph). B: Distribution of the premaxilla-vertebrae angle of 102 fish (X-ray imaging). C: The distribution of snout-bending angles of the L- and R-morphs determined in the field. D: The distribution of premaxilla-vertebrae angles of the L- and R-morphs determined in the field. *T*-test was used to test the significance of the differences between the two morphs, the *P*-value is shown in the figure. E: Correlation between snout-bending angle and premaxilla-vertebrae angle. The Pearson correlation coefficient (r) and its *P*-value are shown in the corner. ns: Not significant.

analysis were carried out on a subsample of 20 extremely asymmetric and 20 near-symmetric fish, as defined by X-ray imaging (Supplementary Figure S2). The 3D reconstruction enabled the isolation of specific ossified units (Figure 2). By examining bones that directly contact prey in lateralized scale eating (premaxilla, maxilla, and mandible; see feeding videos below) and analyzing their relative volumes as indicators of bone size, we identified a consistent pattern of volume discrepancies between left and right sides in most samples (Figure 3A). Specifically, left-headed fish have significantly larger craniofacial bones (premaxilla, maxilla and mandible) on the right side, while right-headed fish have significantly larger bones on the left. Volume asymmetry distributions deviated from a unimodal pattern and fit a bimodal distribution (Figure 3B–D). The Pearson correlation coefficients between these three bone volume asymmetries ranged from 0.75 to 0.88 (*P*-values<0.05). Importantly, significant correlations were observed between all three volume asymmetries and field examination results (*P*-values<0.05; Figure 3E–G). In contrast, no significant correlations (*P*-values>0.05) were found between volume asymmetries and the two primary 2D methods (dorsal photograph and X-ray imaging) (Supplementary Figure S3).

We further assessed bone density on both sides for the bones mentioned above. Among the three clearly separatable bones (see Methods), the maxilla exhibited the highest density, followed by the mandible, and the premaxilla had the lowest (Supplementary Figure S4). Compared to the bilateral asymmetry in bone relative volume, the variation in density was less pronounced (Supplementary Figure S5). Among the bones, the premaxilla showed a significant asymmetry in density, which aligned with the relative volume difference: in the L-morph, the right-side premaxilla was larger and denser and the reverse was true for the R-morph (Supplementary Figure S5). The maxilla also showed a significant density asymmetry, though less pronounced than in the premaxilla. In contrast, the mandible showed no significant asymmetry in density (Supplementary Figure S5).

Major 3D shape variations of head morphology

Our 3D geometric morphometrics analysis revealed that most variations were concentrated in the mandible region (Supplementary Figure S6). The first three shape principal components (PCs), accounted for 63.7%, 7.7%, and 5.8% of the total variance, respectively. Notably, PC1 reflected variations in mouth preservation posture rather than head shape, with smaller PC1 values indicating an open mouth and larger values indicating a closed mouth (Figure 4A; Supplementary Figure S7). To reduce the effect of mouth posture (see Methods) and highlight true shape variations, we adjusted for PC1 and reconducted the PCA analysis.

After adjustments, the original PC2 and PC3 accounted for 21.4% and 16.1% of the total variance, respectively. PC2 primarily correlated with normalized mouth width; smaller PC2 values indicated a broader head, while larger PC2 values indicated a narrowed head (Figure 4A). PC3 was associated with mouth asymmetry: Smaller PC3 values indicated a left-bended head, while larger PC3 values indicated a right-bended head (Figure 4A). The classification of the L- and R-morphs based on the relative volumetric asymmetries was highly consistent with the groups separated by PC3 (Figure 4B), indicating that the adjustment of the bilateral bone volume ultimately leads to bilateral morphological asymmetry.

We then explored the relationships between the morphological traits from the GPA analysis and other factors like body size and sex. Notably, there was a significant correlation (r=0.62; *P*-value<0.05) between normalized mouth width (PC2) and body size (Supplementary Figure S8). However, no significant correlations (*P*-values>0.05) were found between head asymmetry (PC3) and body size or sex (Supplementary Figure S9).

General scale-eating vs. non-scaly eating comparison

To explore if scale-eating behavior contributes to the head asymmetry of *P. microlepis*, we investigate its feeding

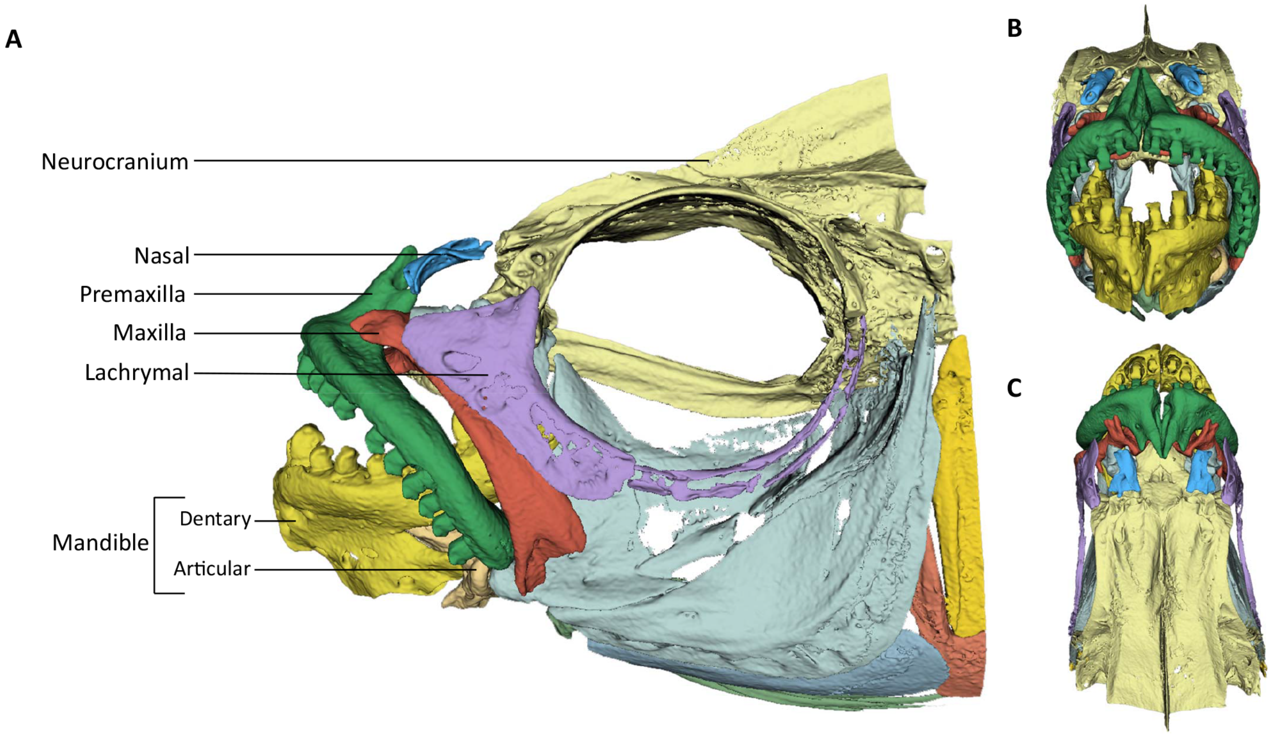

Figure 2 Overall craniofacial skeleton structure of a right-headed scale-eater (*Perissodus microlepis*)

A: Craniofacial structure in lateral view, each color represents a separate ossified unit. B: Craniofacial structure in front view. C: Craniofacial structure in dorsal view.

behavior and kinematics on scales (prey) and non-scaly food. The results show distinct behaviors and kinematics between the two types of food. When consuming non-scaly floating food, the scale-eater gently approached and slightly opened its mouth (Figure 5A; Supplementary Video S1). In contrast, during scale-eating, it initiated an ambush from a considerable distance (~10 cm) and launched a swift attack (~3 cm) from behind and below its prey (Figure 5B; Supplementary Video S2). At around a distance of ~1 cm away from its prey, the scale-eater's body contorted into an S-shape, generating a strong lateral force and opening its mouth widely and asymmetrically to maximize contact with the prey (Figure 5B; Supplementary Video S2). μCT also revealed the structural adaptation of asymmetric bones during mouth opening, highlighting the anatomical modifications that facilitate increased prey contact and efficient scale removal (Figure 5C). Remarkably, the premaxilla and mandible are the bones that come into direct contact with prey and are the first to be impacted during predation (Figure 5B). The consistent increase in the unilateral relative volume and density in the premaxilla not only expands the contact area but also helps prevent damage during significant impacts (Supplementary Figure S5). Nevertheless, the reason why the mandible exhibits significant relative volumetric asymmetry but no density asymmetry requires further investigation.

DISCUSSION

In this study, we assessed the craniofacial skeletal adaptations that facilitate *P. microlepis* to consume scales, using high-resolution μCT imaging combined with high-speed videos. Our results revealed consistent asymmetric craniofacial volume changes, confirming a bimodal, rather than unimodal, distribution. Coupled with high-speed videos, we demonstrated how this fish utilizes asymmetries in both morphology and behavior during the scale-eating process.

Limitations of 2D measurements

Despite both established 2D methodologies (dorsal photograph and X-ray imaging) suggesting a unimodal distribution of head asymmetry, the correlation between them was notably low. Challenges included the environmental distortions during preservation (Cribb & Bray, 2010; Strauss & Bond, 1990) and variations in shooting angles in 2D photographic data (de Menezes et al., 2009; Ghoddousi et al., 2007; Liao et al., 2021; Marquina et al., 2021). Our study illustrates how μCT effectively addresses these limitations, providing a clear example of its contribution to the accurate quantification of this fish morphology.

Insights into bilateral asymmetry innovations in *P. mircolepis*

For decades, both morphological and behavioral asymmetries have intrigued researchers. Our study presents a notable example featuring stable bimodal morphs with balanced frequencies within a population. This is particularly significant given that many previous studies on symmetry breaking have primarily focused on directional asymmetry (or fixed asymmetry), which involves a collective deviation from symmetry, as seen in visceral asymmetry in humans (Levin, 2005), and in over 90% of snail taxa being dextral (Schilthuizen & Davison, 2005). In our research, we reveal for the first time that the head bones of this species exhibit consistent volume asymmetry and a bimodal distribution. Further GM analysis confirms the existence of these two morphs, revealing that this morphological asymmetry results from consistent volume changes in key craniofacial bones and the mutual adjustment between them, leading to an overall deflection of the head. An important area to explore further is whether the morphology of other posterior bones and organs

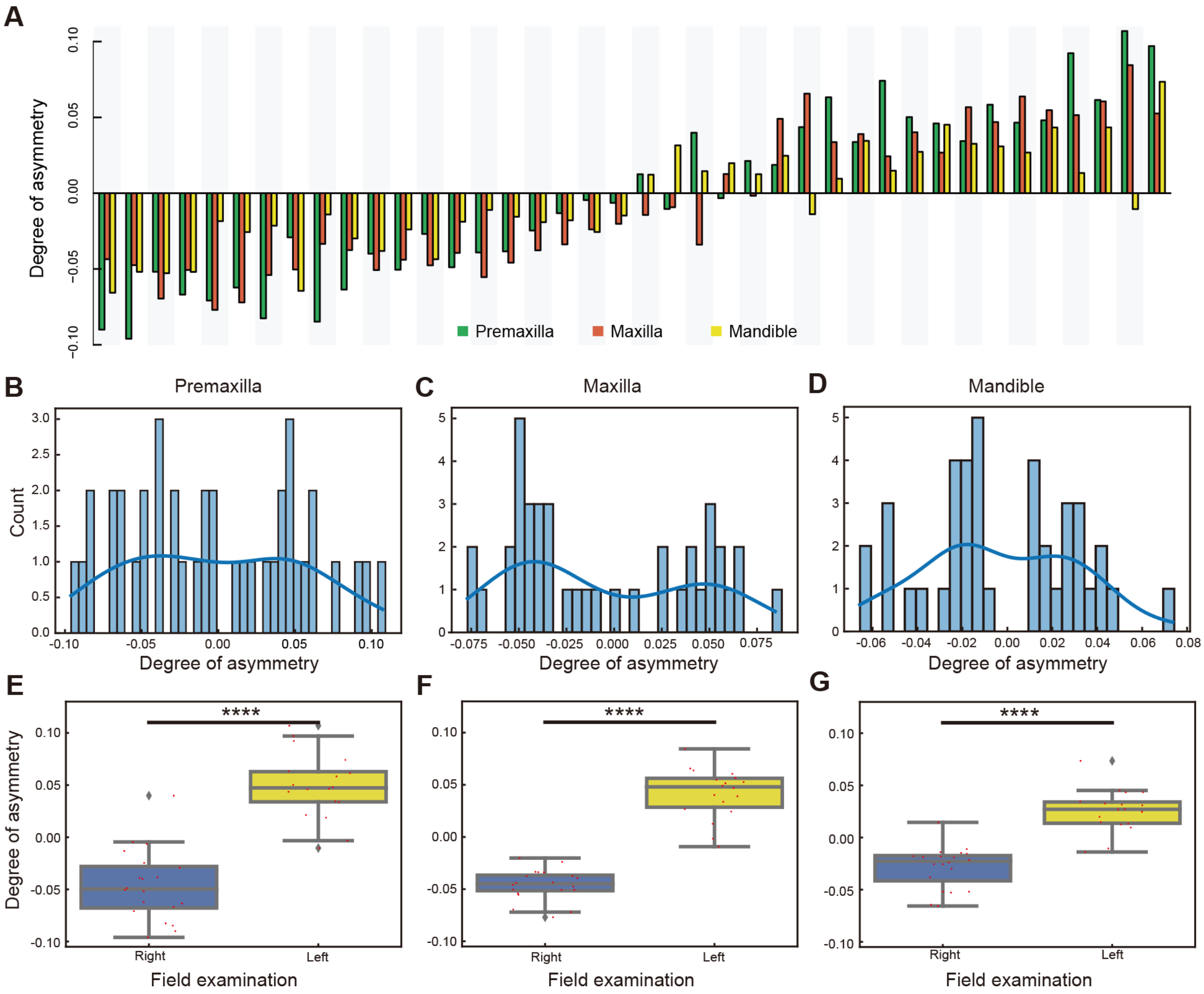

Figure 3 Relative volume asymmetry between left and right sides and its distribution in 40 *Perissodus microlepis*

A: Relative volume differences in skeletons between the left and right sides in 40 individuals are shown. Gray and white columns distinguish each sample, with different skeletons represented by different colors. The green represents the premaxilla, the red represents the maxilla, and the yellow represents the mandible. The relative differences between left and right sides were calculated based on the equation of "Degree of asymmetry=(Left–Right)/(Left+Right)" (Palmer & Strobeck, 1986). In Figure B, C, and D, the distributions of the premaxilla, maxilla, and mandible's degree of relative volumetric asymmetry are displayed, respectively. In Figure E, F, and G, the comparison of relative volumetric asymmetry of the premaxilla, maxilla, and mandible are made between the L- and R-morphs that determined in the field. ns: Not significant; *: $P<0.05$; **: $P<0.01$; ***: $P<0.001$; ****: $P<0.0001$.

conforms to this bimodal distribution, as well as their relationship with jaw bones studied here, including structures like otoliths and the brain. Previous studies have identified a weak negative correlation between the size of the two hemispheres of the brain with the direction of head deflection (Lee et al., 2017). Utilizing both magnetic resonance imaging (MRI) and µCT in the same group of individuals will enable us to establish the potential links.

The adaptations we find in *Perissodus microlepis* align with Liem's (Liem, 1973) theory of cranial evolution in cichlids, where only minor modifications of existing structures are required for successful and rapid adaptation to significant shifts in adaptive zones. For example, species with hypertrophied lips, which have evolved repeatedly across major cichlid radiations, are better suited to exploit food from narrow crevices (Baumgarten et al., 2015). Beyond cichlids, similar structural adaptations—such as premaxilla protrusion and lower jaw depression—enable the largescale foureyes (*Anableps anableps*) to feed on land (Michel et al., 2015). Moreover, our study also hints at bone density differences as adaptations for asymmetric usage in *P. microlepis* that may enable high-speed attacks without bone damage and higher feeding efficiency. Comparing jaw and tooth density across species, particularly with non-scale-eating relatives, could provide deeper insights into the evolutionary and functional significance of these adaptations and the developmental and evolutionary paths that led to the apparent adaptive differences of this trait.

Potential implications of this high-quality morphological data

The 3D µCT analysis reveals that head asymmetry in *P. microlepis* is a continuous trait with a bimodal distribution. A next focus could be to explore its potential genetic basis. We proposed three hypotheses. First, like other dimorphic traits, such as the coexistence of gold and dark morphs in Midas cichlids (*Amphilophus* spp.) (Kautt et al., 2020; Kratochwil et al., 2022) and dorsal spine polymorphism in stickleback (*Apeltes quadracus*) (Wucherpfennig et al., 2022), the bilateral head asymmetry of this fish might be determined by a single

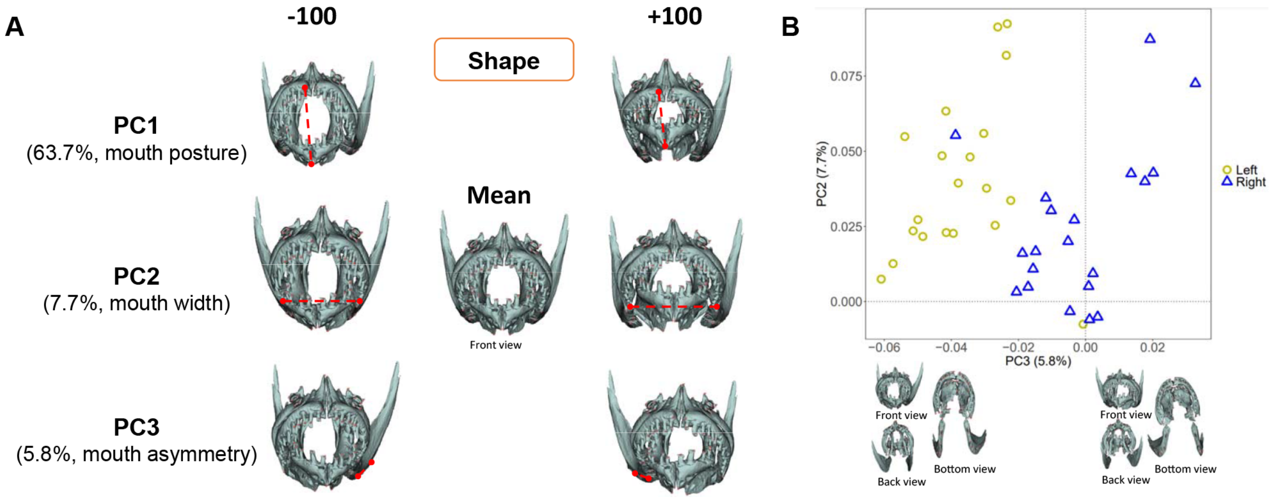

Figure 4 Major 3D shape variations in the heads of 40 *Perissodus microlepis* individuals

A: Virtual heads with PC values deviating from the mean by ±100. Red dotted lines indicate variations in shape. B: Scatter plots illustrating PC2 and PC3. The classification of L- and R- morphs for the samples was determined based on independent volume disparities between the left and right sides (refer to Figure 3A). Yellow denotes L-morph, while blue represents R-morph.

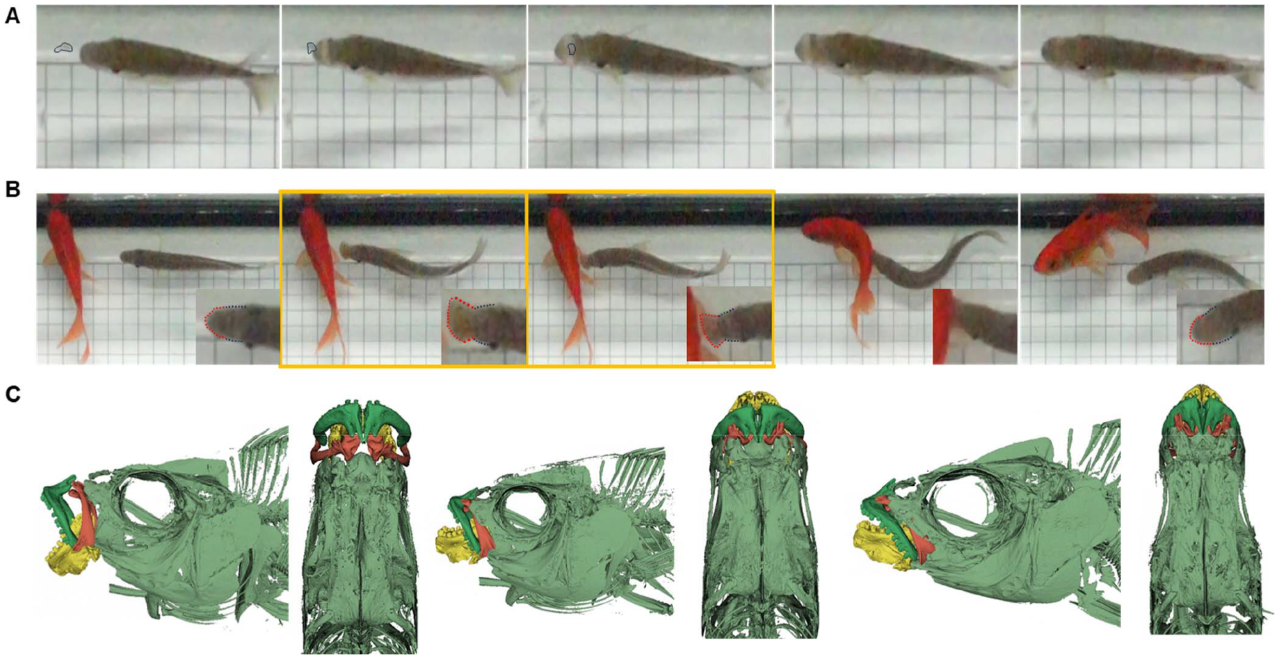

Figure 5 Mouth and internal skeleton deformation

A, B: Kinematic high-speed video images of feeding events. Each frame illustrates a representative stage within the feeding events. A: Capture feeding on mysis. The food source is outlined. B: The scraping behavior of scale-eating. The changes in the outline of the mouth are indicated by red dotted lines. The black dotted line is used as a contrast. C: The lateral and dorsal views of fish that are preserved in ethanol with different levels of opening and closing of the mouth. Key skeletal parts including premaxilla, maxilla, and mandible are marked in intense green, red, and yellow, respectively.

(or very few) major effect loci, with phenotypic plasticity explaining the variation around the bimodal peaks. Secondly, behavioral laterality, which in itself presumably has a genetic basis, shapes head asymmetry through developmental plasticity (Neufeld & Palmer, 2011; Palmer, 2004, 2010; Van Dooren et al., 2010). Lastly, it seems most likely that both the lateralized feeding preference, which manifests itself quite early in ontogeny (Meyer lab, unpublished data), and morphological asymmetry (genetic basis) reinforce each other and become more pronounced as the fish grows (developmental plasticity). Overall, there are likely to exist a set of influential genetic loci that contribute measurably to the asymmetry observed in head morphology. But, this needs further exploration.

In conclusion, our study contibutes to clarifying the distribution of head asymmetry in this fish species. The fish develops bilateral morphological asymmetry through volume changes in key craniofacial bones, resulting in a bimodal distribution in the population. Furthermore, using *P. microlepis* as a case study, it illustrates how fish explore new ecological niches through coordinated innovations in morphology and behavior. By providing high-quality phenotypic data, this research establishes a solid foundation for future genetic research.

SUPPLEMENTARY DATA

Supplementary data to this article can be found online.

COMPETING INTERESTS

The authors declare that they have no competing interests.

AUTHORS' CONTRIBUTIONS

X.T.: Conceptualization, Data collection, Formal analysis, Visualization, Writing the original and final draft, Funding acquisition. S.L: Data collection of µCT, Review & Editing of the manuscript. J.T.: Data collection of µCT and Funding acquisition. A.M.: Conceptualization, Supervision, Formal analysis, Review & Editing of the manuscript, Funding acquisition. All authors read and approved the final version of the manuscript.

ACKNOWLEDGEMENTS

We thank Jan Gerwin for his help in collecting fish in Zambia 2018. We are grateful to the scientific computing cluster (SCC) and the animal research facility (TFA) of the University of Konstanz; and the University of Ulm for their assistance with µCT. We thank Ryan Greenway, Ming Li, Nicolás Roberto Ehemann and Christopher Darrin Hulsey for useful discussions. We thank Nadja Günther for assistance in the laboratory.

REFERENCES

Baumgarten L, Machado-Schiaffino G, Henning F, et al. 2015. What big lips are good for: on the adaptive function of repeatedly evolved hypertrophied lips of cichlid fishes. *Biological Journal of the Linnean Society*, **115**(2): 448–455.

Berlinghieri F, Panizzon P, Penry-Williams IL, et al. 2021. Laterality and fish welfare - A review. *Applied Animal Behaviour Science*, **236**: 105239.

Cribb TH, Bray RA. 2010. Gut wash, body soak, blender and heat-fixation: approaches to the effective collection, fixation and preservation of trematodes of fishes. *Systematic Parasitology*, **76**(1): 1–7.

de Menezes M, Rosati R, Allievi C, et al. 2009. A photographic system for the three-dimensional study of facial morphology. *The Angle Orthodontist*, **79**(6): 1070–1077.

Fedorov A, Beichel R, Kalpathy-Cramer J, et al. 2012. 3D Slicer as an image computing platform for the Quantitative Imaging Network. *Magnetic Resonance Imaging*, **30**(9): 1323–1341.

Futuyma DJ. 2009. Evolution. 2nd ed. Sunderland: Sinauer Associates.

Ghoddousi H, Edler R, Haers P, et al. 2007. Comparison of three methods of facial measurement. *International Journal of Oral and Maxillofacial Surgery*, **36**(3): 250–258.

Gower JC. 1975. Generalized procrustes analysis. *Psychometrika*, **40**(1): 33–51.

Hata H, Yasugi M, Takeuchi Y, et al. 2013. Measuring and evaluating morphological asymmetry in fish: distinct lateral dimorphism in the jaws of scale-eating cichlids. *Ecology and Evolution*, **3**(14): 4641–4647.

Hori M. 1993. Frequency-dependent natural selection in the handedness of scale-eating cichlid fish. *Science*, **260**(5105): 216–219.

Hori M, Ochi H, Kohda M. 2007. Inheritance pattern of lateral dimorphism in two cichlids (a scale eater, *Perissodus microlepis*, and an herbivore, *Neolamprologus moorii*) in Lake Tanganyika. *Zoological Science*, **24**(5): 486–492.

Indermaur A, Theis A, Egger B, et al. 2018. Mouth dimorphism in scale-eating cichlid fish from Lake Tanganyika advances individual fitness. *Evolution*, **72**(9): 1962–1969.

Kautt AF, Kratochwil CF, Nater A, et al. 2020. Contrasting signatures of genomic divergence during sympatric speciation. *Nature*, **588**(7836): 106–111.

Kawano S, Connell JH, Hidaka T. 1987. Evolution and Coadaptation in Biotic Communities. Tokyo: University of Tokyo Press.

Keenleyside MH. 1991. Cichlid Fishes: Behaviour, Ecology and Evolution. Dordrecht: Springer.

Kratochwil CF, Kautt AF, Nater A, et al. 2022. An intronic transposon insertion associates with a trans-species color polymorphism in Midas cichlid fishes. *Nature Communications*, **13**(1): 296.

Kusche H, Lee HJ, Meyer A. 2012. Mouth asymmetry in the textbook example of scale-eating cichlid fish is not a discrete dimorphism after all. *Proceedings of the Royal Society B: Biological Sciences*, **279**(1748): 4715–4723.

Lee HJ, Heim V, Meyer A. 2015. Genetic and environmental effects on the morphological asymmetry in the scale-eating cichlid fish, *Perissodus microlepis*. *Ecology and Evolution*, **5**(19): 4277–4286.

Lee HJ, Kusche H, Meyer A. 2012. Handed foraging behavior in scale-eating cichlid fish: its potential role in shaping morphological asymmetry. *PLoS One*, **7**(9): e44670.

Lee HJ, Pittlik S, Jones JC, et al. 2010. Genetic support for random mating between left and right-mouth morphs in the dimorphic scale-eating cichlid fish *Perissodus microlepis* from Lake Tanganyika. *Journal of Fish Biology*, **76**(8): 1940–1957.

Lee HJ, Schneider RF, Manousaki T, et al. 2017. Lateralized feeding behavior is associated with asymmetrical neuroanatomy and lateralized gene expressions in the brain in scale-eating cichlid fish. *Genome Biology and Evolution*, **9**(11): 3122–3136.

Levin M. 2005. Left-right asymmetry in embryonic development: a comprehensive review. *Mechanisms of Development*, **122**(1): 3–25.

Liao YH, Zhou CW, Liu WZ, et al. 2021. 3DPhenoFish: application for two- and three-dimensional fish morphological phenotype extraction from point cloud analysis. *Zoological Research*, **42**(4): 492–502.

Liem KF. 1973. Evolutionary strategies and morphological innovations: cichlid pharyngeal jaws. *Systematic Biology*, **22**(4): 425–441.

Liem KF, Stewart DJ. 1976. Evolution of the scale-eating cichlid fishes of Lake Tanganyika: a generic revision with a description of a new species. *Bulletin of the Museum of Comparative Zoology*, **147**(7): 319–350.

Marquina D, Buczek M, Ronquist F, et al. 2021. The effect of ethanol concentration on the morphological and molecular preservation of insects for biodiversity studies. *PeerJ*, **9**: e10799.

Michel KB, Aerts P, Gibb AC, et al. 2015. Functional morphology and kinematics of terrestrial feeding in the largescale foureyes (*Anableps anableps*). *Journal of Experimental Biology*, **218**(Pt 18): 2951–2960.

Neufeld CJ, Palmer AR. 2011. Learning, developmental plasticity, and the rate of morphological evolution. *In*: Hallgrimsson B, Hall BK. Epigenetics: Linking Genotype and Phenotype in Development and Evolution. Berkeley: University of California Press.

Nijhout HF, Davidowitz G. 2003. Developmental perspectives on phenotypic variation, canalization, and fluctuating asymmetry. *In*: Polak M. Developmental Instability: Causes and Consequences. New York: Oxford University Press, 3–13.

Palmer AR. 2004. Symmetry breaking and the evolution of development. *Science*, **306**(5697): 828–833.

Palmer AR. 2010. Scale-eating cichlids: from hand(ed) to mouth. *Journal of Biology*, **9**(2): 11.

Palmer AR, Strobeck C. 1986. FLUCTUATING ASYMMETRY: measurement, analysis, patterns. *Annual Review of Ecology and Systematics*, **17**: 391–421.

Pearson K. 1900. X. On the criterion that a given system of deviations from the probable in the case of a correlated system of variables is such that it can be reasonably supposed to have arisen from random sampling. *The London, Edinburgh, and Dublin Philosophical Magazine and Journal of Science*, **50**(302): 157–175.

Pearson K. 1901. LIII. On lines and planes of closest fit to systems of points in space. *The London, Edinburgh, and Dublin Philosophical Magazine and Journal of Science*, **2**(11): 559–572.

Pither J, Taylor PD. 2000. Directional and fluctuating asymmetry in the black-winged damselfly *Calopteryx maculata* (Beauvois) (Odonata: Calopterygidae). *Canadian Journal of Zoology*, **78**(10): 1740–1748.

Raffini F, Fruciano C, Franchini P, et al. 2017. Towards understanding the genetic basis of mouth asymmetry in the scale-eating cichlid *Perissodus microlepis*. *Molecular Ecology*, **26**(1): 77–91.

Raffini F, Fruciano C, Meyer A. 2018. Gene(s) and individual feeding behavior: exploring eco-evolutionary dynamics underlying left-right asymmetry in the scale-eating cichlid fish *Perissodus microlepis*. *Ecology and Evolution*, **8**(11): 5495–5507.

Raffini F, Meyer A. 2019. A comprehensive overview of the developmental basis and adaptive significance of a textbook polymorphism: head asymmetry in the cichlid fish *Perissodus microlepis*. *Hydrobiologia*, **832**(1): 65–84.

Rohlf FJ. 2006a. tpsDig, Digitize Landmarks and Outlines, version 2.05. Stony Brook, NY: Department of Ecology and Evolution, State University of New York.

Rohlf FJ. 2006b. tpsUtil, version 1.38. http://life. bio. sunysb. edu/morph/index. Html.

Rohlf FJ, Slice D. 1990. Extensions of the procrustes method for the optimal superimposition of landmarks. *Systematic Biology*, **39**(1): 40–59.

Schilthuizen M, Davison A. 2005. The convoluted evolution of snail chirality. *Naturwissenschaften*, **92**(11): 504–515.

Sommer-Trembo C, Santos ME, Clark B, et al. 2024. The genetics of niche-specific behavioral tendencies in an adaptive radiation of cichlid fishes. *Science*, **384**(6694): 470–475.

Stewart TA, Albertson RC. 2010. Evolution of a unique predatory feeding apparatus: functional anatomy, development and a genetic locus for jaw laterality in Lake Tanganyika scale-eating cichlids. *BMC Biology*, **8**: 8.

Strauss RE, Bond CE. 1990. Taxonomic methods: morphology. *In*: Schreck CB, Moyle PB. Methods for Fish Biology. Bethesda: American Fisheries Society, Special Publication, 109–140.

Takahashi R, Watanabe K, Nishida M, et al. 2007. Evolution of feeding specialization in Tanganyikan scale-eating cichlids: a molecular phylogenetic approach. *BMC Evolutionary Biology*, **7**: 195.

Takeuchi Y, Hata H, Maruyama A, et al. 2019. Specialized movement and laterality of fin-biting behaviour in *Genyochoromis mento* in Lake Malawi. *Journal of Experimental Biology*, **222**(Pt 3): jeb191676.

Takeuchi Y, Higuchi Y, Ikeya K, et al. 2022. Experience-dependent learning of behavioral laterality in the scale-eating cichlid *Perissodus microlepis* occurs during the early developmental stage. *Scientific Reports*, **12**(1): 723.

Takeuchi Y, Hori M, Oda Y. 2012. Lateralized kinematics of predation behavior in a Lake Tanganyika scale-eating cichlid fish. *PLoS One*, **7**(1): e29272.

Takeuchi Y, Hori M, Tada S, et al. 2016. Acquisition of lateralized predation behavior associated with development of mouth asymmetry in a lake tanganyika scale-eating cichlid fish. *PLoS One*, **11**(1): e0147476.

Takeuchi Y, Ishikawa A, Oda Y, et al. 2018. Lateralized expression of left-right axis formation genes is shared by adult brains of lefty and righty scale-eating cichlids. *Comparative Biochemistry and Physiology Part D: Genomics and Proteomics*, **28**: 99–106.

Takeuchi Y, Oda Y. 2017. Lateralized scale-eating behaviour of cichlid is acquired by learning to use the naturally stronger side. *Scientific Reports*, **7**(1): 8984.

Van Dooren TJM, Van Goor HA, Van Putten M. 2010. Handedness and asymmetry in scale-eating cichlids: antisymmetries of different strength. *Evolution*, **64**(7): 2159–2165.

Van Rossum G, Drake FL. 2009. Python/C Api Manual-Python 3. Scotts Valley: CreateSpace.

Wucherpfennig JI, Howes TR, Au JN, et al. 2022. Evolution of stickleback spines through independent *cis*-regulatory changes at *HOXDB*. *Nature Ecology & Evolution*, **6**(10): 1537–1552.